



Pseudorapidity density of charged particles in p–Pb collisions at sNN = 5.02 TeV

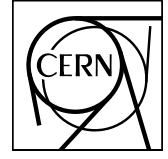
Abelev, B.; Adam, J.; Adamová, D.; Bearden, Ian; Bilandzic, Ante; Bøggild, Hans; Chojnacki, Marek; Christensen, Christian Holm; Dalsgaard, Hans Hjørning; Gaardhøje, Jens Jørgen; Gulbrandsen, Kristjan Herlache; Hansen, Alexander Colliander; Nielsen, Børge Svane; Nygaard, Casper; Søgaard, Carsten; Zaccolo, Valentina

Published in:
arXiv.org: Physics

Publication date:
2012

Document version
Publisher's PDF, also known as Version of record

Citation for published version (APA):
Abelev, B., Adam, J., Adamová, D., Bearden, I., Bilandzic, A., Bøggild, H., Chojnacki, M., Christensen, C. H., Dalsgaard, H. H., Gaardhøje, J. J., Gulbrandsen, K. H., Hansen, A. C., Nielsen, B. S., Nygaard, C., Søgaard, C., & Zaccolo, V. (2012). Pseudorapidity density of charged particles in p–Pb collisions at sNN = 5.02 TeV. *arXiv.org: Physics*, (arXiv:1210.3615). <http://arxiv.org/pdf/1210.3615.pdf>



CERN-PH-EP-2012-307
08 Oct 2012

Pseudorapidity density of charged particles in p–Pb collisions at $\sqrt{s_{NN}} = 5.02$ TeV

ALICE Collaboration*

Abstract

The charged-particle pseudorapidity density measured over 4 units of pseudorapidity in non-single-diffractive (NSD) p–Pb collisions at a centre-of-mass energy per nucleon pair $\sqrt{s_{NN}} = 5.02$ TeV is presented. The average value at midrapidity is measured to be 16.81 ± 0.71 (*syst.*), which corresponds to 2.14 ± 0.17 (*syst.*) per participating nucleon, calculated with the Glauber model. This is 16% lower than in NSD pp collisions interpolated to the same collision energy, and 84% higher than in d–Au collisions at $\sqrt{s_{NN}} = 0.2$ TeV. The measured pseudorapidity density in p–Pb collisions is compared to model predictions, and provides new constraints on the description of particle production in high-energy nuclear collisions.

arXiv:1210.3615v2 [nucl-ex] 25 Feb 2013

*See Appendix A for the list of collaboration members

Particle production in proton–lead collisions, in contrast to pp, is expected to be sensitive to nuclear effects in the initial state. In particular, coherence effects in the nuclear wave function are expected to influence the initial parton flux, as well as the underlying description of particle production in the scattering processes. Therefore, measurements in p–Pb collisions at the Large Hadron Collider (LHC) at CERN provide an essential experimental tool to discriminate between the initial and final state effects, and allow one to attribute the latter to the formation of hot QCD matter in heavy-ion collisions [1]. Moreover, at LHC energies, the nuclear wave function is probed at small parton fractional momentum x . The growth of the parton densities with decreasing x must be limited to satisfy unitarity bounds. One of the mechanisms providing such a limitation is often referred to as gluon saturation. Its theoretical description varies between models of particle production resulting in significant differences in the predictions of the charged-particle pseudorapidity density. Thus, the measurements of particle production in p–Pb collisions constrain and potentially exclude certain models, and enhance the understanding of QCD at small x and the initial state.

In this letter, the measurement of the primary charged-particle pseudorapidity density in p–Pb collisions at a nucleon–nucleon centre-of-mass energy $\sqrt{s_{\text{NN}}} = 5.02$ TeV with the ALICE detector [2] is reported. The primary charged-particle density, $dN_{\text{ch}}/d\eta_{\text{lab}}$, is measured in non single-diffractive (NSD) p–Pb collisions for $|\eta_{\text{lab}}| < 2$, where $\eta_{\text{lab}} = -\ln \tan(\theta/2)$ and θ is the polar angle between the charged-particle direction and the beam axis (z). Primary particles are defined as prompt particles produced in the collision, including decay products, except those from weak decays of strange particles. The data are compared to model predictions [3–7], and to measurements in proton–nucleus [8, 9], NSD [10–16], and inelastic [17–20] pp ($p\bar{p}$), as well as central heavy-ion [20–31] collisions.

The p–Pb collisions were provided by the LHC during a short pilot run performed in September 2012 in preparation for the p–Pb physics run scheduled for the beginning of 2013. The two-in-one magnet design of the LHC imposes the same magnetic rigidity of the beams in the two rings. Beam 1 consisted of protons at 4 TeV energy circulating in the negative z -direction in the ALICE laboratory system, while beam 2 consisted of fully stripped $^{208}_{82}\text{Pb}$ ions at 82×4 TeV energy circulating in the positive z -direction. This configuration resulted in collisions at $\sqrt{s_{\text{NN}}} = 5.02$ TeV in the nucleon–nucleon centre-of-mass system, which moves with a rapidity of $\Delta y_{\text{NN}} = 0.465$ in the direction of the proton beam.

The main detector for the present analysis is the Silicon Pixel Detector (SPD), located in the inner barrel of the ALICE detector inside a solenoidal magnet providing a magnetic field of 0.5 T. The SPD consists of two cylindrical layers of hybrid silicon pixel assemblies covering $|\eta_{\text{lab}}| < 2.0$ for the inner layer and $|\eta_{\text{lab}}| < 1.4$ for the outer layer with respect to vertices at the nominal interaction point. A total of 9.8×10^6 pixels of size $50 \times 425 \mu\text{m}^2$ are read out, of which 93.5% were active during the run. The primary trigger signal was provided by the VZERO counters, two arrays of 32 scintillator tiles each covering the full azimuth within $2.8 < \eta_{\text{lab}} < 5.1$ (VZERO-A) and $-3.7 < \eta_{\text{lab}} < -1.7$ (VZERO-C). The signal amplitude and arrival time collected in each scintillator are recorded. The time resolution is better than 1 ns, allowing discrimination of beam–beam collisions from background events produced outside of the interaction region. Additionally, two neutron Zero Degree Calorimeters (ZDCs) are used, which are located at +112.5 m (ZNA) and –112.5 m (ZNC) from the interaction point. Their energy resolution is about 20% for single neutrons with a few TeV energy. Each ZDC also provided a trigger with high efficiency for single neutrons, which was used to collect a control sample of events for the estimation of the efficiency of the VZERO trigger.

During the run, beams consisting of 13 bunches were circulating, with about 10^{10} protons and 6×10^7 Pb ions per bunch. In the ALICE interaction region, 8 pairs of bunches were colliding, leading to a luminosity of $8 \times 10^{25} \text{ cm}^{-2}\text{s}^{-1}$. The luminous region had a r.m.s. width of 6.3 cm in the z -direction and about $60 \mu\text{m}$ in the transverse direction. The trigger was configured for high efficiency for hadronic events, requiring a signal in either VZERO-A or VZERO-C. This configuration led to an observed trigger rate of about 200 Hz with a hadronic collision rate of about 150 Hz. In the offline analysis, a signal is

required in both VZERO-A and VZERO-C. Beam–gas and other machine-induced background triggers with deposited energy above the thresholds in the VZERO or ZDC detectors are suppressed by requiring the arrival time to be compatible with that of a nominal p–Pb interaction. The contamination from background is estimated from control triggers on non-colliding bunches, and found to be negligible.

In principle, the event sample obtained after these requirements consists of NSD collisions as well as single-diffractive (SD) and electromagnetic (EM) interactions. The efficiency of the trigger and event selection on the different processes is estimated using a combination (cocktail) of the following Monte Carlo (MC) event generators: a) DPMJET [32] for NSD p–Pb interactions, b) PHOJET [33] tuned to pp data at $\sqrt{s_{NN}} = 2.76$ and 7 TeV [34] together with a Glauber model [35] for the contribution from SD interactions, and c) STARLIGHT [36] used together with PYTHIA [37] or PHOJET [33] for the proton excitation in the electromagnetic field of the $^{208}_{82}\text{Pb}$ nucleus. The DPMJET [32] generator, which is based on the Gribov-Glauber approach and treats soft and hard scattering processes in an unified way, includes incoherent SD collisions of the projectile proton with target nucleons that are concentrated mainly on the surface of the nucleus. These are removed by requiring that at least one of the binary nucleon–nucleon interactions is NSD. The relative weight of the events in the cocktail is given by the cross sections of the corresponding processes, which are taken to be 2.0 b (0.1 b) for NSD (SD) collisions (estimated from the Glauber model), and 0.1–0.2 b for EM interactions (estimated from STARLIGHT calculations). The detector response to the cocktail is simulated using a model of the ALICE detector and the GEANT3 simulation tool [38]. An efficiency of 99.2% for NSD collisions and a negligible contamination from SD and EM interactions are obtained.

From the collected data sample used for the analysis, 0.8×10^6 events pass the selection criteria. Among the selected events, 98.5% are found to have a primary vertex. The corresponding fraction in DPMJET [32] for NSD collisions is 99.4% with the probability of selecting an event without a primary vertex of 41%. Taking into account the difference of the fraction of events without vertex in the data and the simulation results in an overall selection efficiency of 96.4% for NSD events entering the analysis.

The $dN_{\text{ch}}/d\eta_{\text{lab}}$ analysis techniques employed are identical to those described in Ref. [29], where the similar measurement is reported for Pb–Pb collisions. Events are selected with a reconstructed vertex within $|z_{\text{vtx}}| < 18$ cm, which results in a $|\eta_{\text{lab}}| < 2$ coverage for the $dN_{\text{ch}}/d\eta_{\text{lab}}$ measurement. Tracklet candidates are formed using the position of the primary vertex and two hits, one on each SPD layer. From these candidates, tracklets are selected by a requirement on the sum of the squares of the differences (residuals) in azimuthal and polar angles relative to the primary vertex for each hit, effectively selecting charged particles with transverse momentum (p_{T}) above 50 MeV/c, while particles below 50 MeV/c are mostly absorbed by detector material. The charged-particle pseudorapidity density is then obtained from the measured distribution of tracklets $dN_{\text{tracklets}}/d\eta_{\text{lab}}$ as $dN_{\text{ch}}/d\eta_{\text{lab}} = \alpha(1 - \beta)dN_{\text{tracklets}}/d\eta_{\text{lab}}$. The correction α accounts for the acceptance and efficiency for a primary particle to produce a tracklet, while β is the contamination of reconstructed tracklets from combinations of hits not produced by the same primary particle. Both are determined as a function of the z -position of the primary vertex and the pseudorapidity of the tracklet from detector simulations using DPMJET [32] and GEANT3 [38], and found to be on average 1.2 and 0.01, respectively. Since the corrections applied in the analysis implicitly only account for the fraction of events without vertex given by the simulation, the $dN_{\text{ch}}/d\eta_{\text{lab}}$ is further corrected by -2.2% for the difference of this fraction in the data and the simulation.

The following sources of systematic uncertainties have been considered. The uncertainty in detector acceptance is estimated to be 1.5% determined from the change of the multiplicity at a given η_{lab} by varying the range of the z -position of the vertex. The uncertainties resulting from the subtraction of the combinatorial background and from the contribution of weak decays are estimated to be 0.3% and 0.8%, respectively. They are determined from the comparison in data and simulation of the tracklet residual distributions, in which the tails are dominated by combinatorial background and secondaries. The uncertainty due to the particle composition is estimated to be 1%, which was determined by changing

the relative abundances of pions, kaons and protons by a factor of 2 in the simulation. The uncertainty due to the correction down to zero p_T is estimated to be 1% by varying the amount of undetected particles at low p_T by 50%. The uncertainty related to the trigger and event selection efficiency for NSD collisions is estimated to be 3.1% using a small sample of events collected with the ZNA trigger with an offline selection on the deposited energy corresponding to approximately 12 neutrons from the Pb remnant. The value used for the threshold has been determined from DPMJET with associated nuclear fragment production [39], and was chosen to suppress the contamination of the EM and SD interactions. In total, a systematic uncertainty of about 3.8% is obtained by adding in quadrature all the contributions.

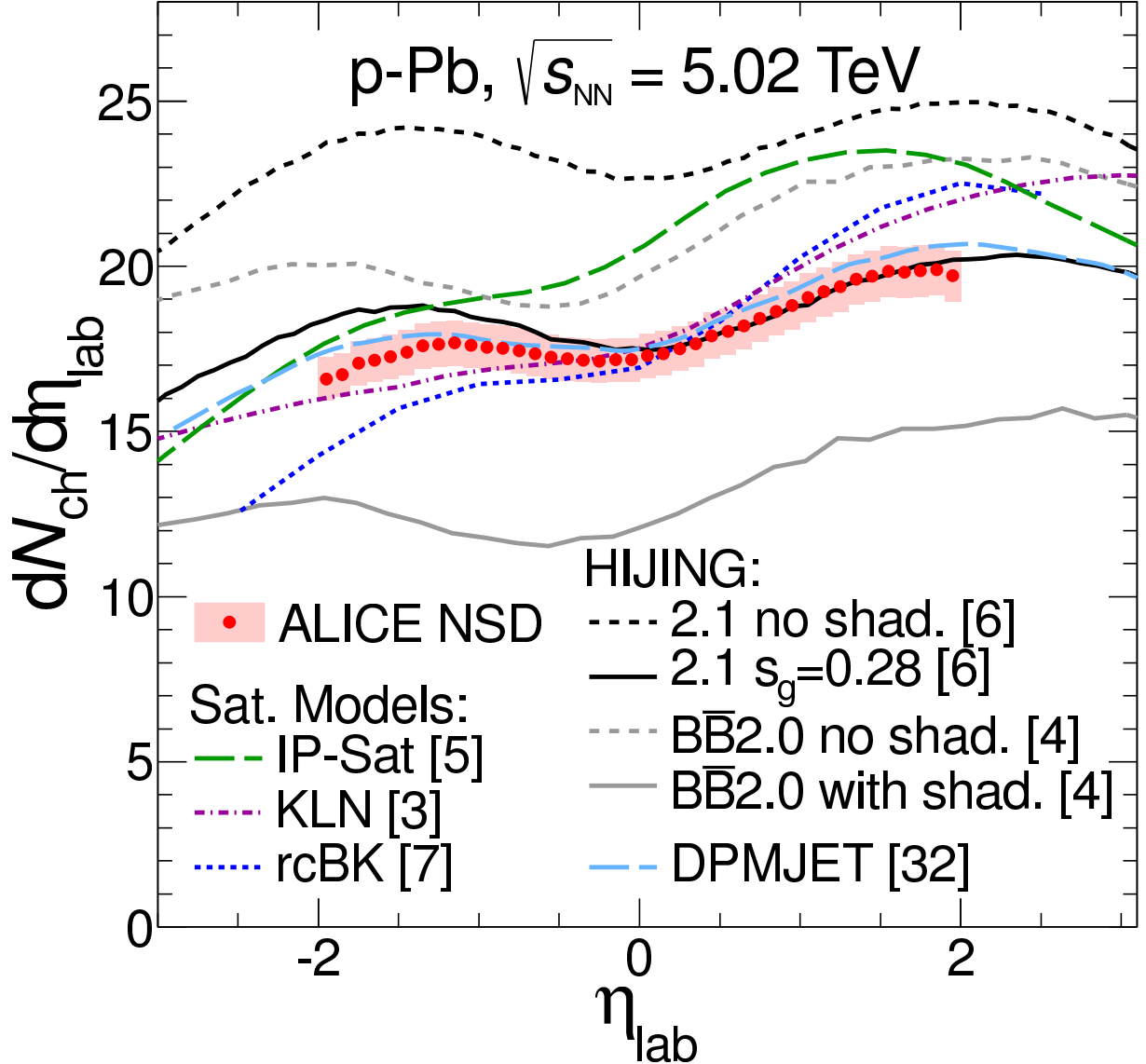


Fig. 1: Pseudorapidity density of charged particles measured in NSD p–Pb collisions at $\sqrt{s_{NN}} = 5.02$ TeV compared to theoretical predictions [3–7]. The calculations [4, 5] have been shifted to the laboratory system.

The resulting pseudorapidity density is presented in Fig. 1 for $|\eta_{lab}| < 2$. A forward–backward asymmetry between the proton and lead hemispheres is clearly visible. The measurement is compared to particle production models [3–7] that describe similar measurements in other collision systems [9, 20–31]. The two-component models [4, 6] combine perturbative QCD processes with soft interactions, and include nuclear modification of the initial parton distributions. The saturation models [3, 5, 7] employ coher-

	$dN_{\text{ch}}/d\eta_{\text{lab}}$			$\frac{dN_{\text{ch}}/d\eta_{\text{lab}} _{\eta_{\text{lab}}=2.0}}{dN_{\text{ch}}/d\eta_{\text{lab}} _{\eta_{\text{lab}}=-2.0}}$
	-2.0	0.0	2.0	
ALICE	16.65 ± 0.65	17.24 ± 0.66	19.81 ± 0.78	1.19 ± 0.05
Saturation Models				
IP-Sat [5]	17.55	20.55	23.11	1.32
KLN [3]	15.96	17.51	22.02	1.38
rcBK [7]	14.27	16.94	22.51	1.58
HIJING				
2.1 no shad. [6]	23.58	22.67	24.96	1.06
2.1 $s_g = 0.28$ [6]	18.30	17.49	20.21	1.10
B $\bar{\text{B}}$ 2.0 no shad. [4]	20.03	19.68	23.24	1.16
B $\bar{\text{B}}$ 2.0 with shad. [4]	12.97	12.09	15.16	1.17
DPMJET [32]	17.50	17.61	20.67	1.18

Table 1: Comparison of the pseudorapidity distribution between data and the models at $\eta_{\text{lab}} = -2, 0$ and 2 (integrated in 0.2 units of pseudorapidity) as well as the ratio of $dN_{\text{ch}}/d\eta_{\text{lab}}$ at $\eta_{\text{lab}} = 2$ to that at $\eta_{\text{lab}} = -2$. The uncertainty introduced by taking the ratio neglecting the Jacobian amounts to about 2 and 6% estimated for the saturation and HIJING models, respectively.

ence effects to reduce the number of soft gluons available for particle production below a given energy scale. The calculations [3, 6, 7] at $\sqrt{s_{\text{NN}}} = 5.02$ TeV were provided by the authors in the laboratory system. The calculations that were performed in the centre-of-mass system [4, 5] have been shifted by Δy_{NN} into the ALICE laboratory system. For low- p_{T} particles, this is only an approximation of a Lorentz transformation. In the η_{lab} -range of our measurement, the error on the $dN_{\text{ch}}/d\eta_{\text{lab}}$ density induced by this procedure is estimated using the HIJING model [40], and found to be below 6% . It is worth noting that the HIJING calculations include single-diffraction, which from the HIJING generator [40] is estimated to be about 4% . A comparison of the model calculations with the data shows that most of the models that include shadowing [6] or saturation [3, 7] predict the measured multiplicity values to within 20% (see also Tab. 1). The HIJING/B $\bar{\text{B}}$ 2.0 [4] model, which uses an energy and nuclear thickness dependent string tension to mimic the effect of strong longitudinal color fields, predicts values below the data when including shadowing, and above the data when excluding shadowing. DPMJET [32] (normalized to NSD) and HIJING 2.1 [6], where the gluon shadowing parameter $s_g = 0.28$ was tuned to describe experimental data on rapidity distributions in d–Au collisions at $\sqrt{s_{\text{NN}}} = 0.2$ TeV (RHIC) [9, 20], give values that are closest to the data. Both also describe the pseudorapidity shape relatively well, whereas the saturation models [3, 5, 7] exhibit a steeper η_{lab} dependence than the data. This can also be seen in Tab. 1 by quantifying the density at midrapidity, near the proton and lead peak regions, as well as the ratio of $dN_{\text{ch}}/d\eta_{\text{lab}}$ at $\eta_{\text{lab}} = 2$ to that at $\eta_{\text{lab}} = -2$, for the data (integrated in 0.2 units of pseudorapidity) and the models. The error introduced by taking the ratio amounts to about 2 and 6% for the saturation and HIJING models.

The charged-particle pseudorapidity density at midrapidity in the laboratory system ($|\eta_{\text{lab}}| < 0.5$) is $dN_{\text{ch}}/d\eta_{\text{lab}} = 17.35 \pm 0.01$ (*stat.*) ± 0.67 (*syst.*). The statistical uncertainty is neglected in the following. To obtain the pseudorapidity density in the centre-of-mass system, the data is integrated in the range $-0.965 < \eta_{\text{lab}} < 0.035$, and corrected for the effect of the Δy shift. The correction is estimated from the HIJING model [40] to be 3% , with an uncertainty of 1.5% , added in quadrature to the systematic uncertainty. The resulting pseudorapidity density in the nucleon–nucleon centre-of-mass system is $dN_{\text{ch}}/d\eta_{\text{cms}} = 16.81 \pm 0.71$ (*syst.*).

In order to compare bulk particle production in different collision systems, the charged particle density is scaled by the number of participating nucleons, determined using the Glauber model [35] with a nuclear

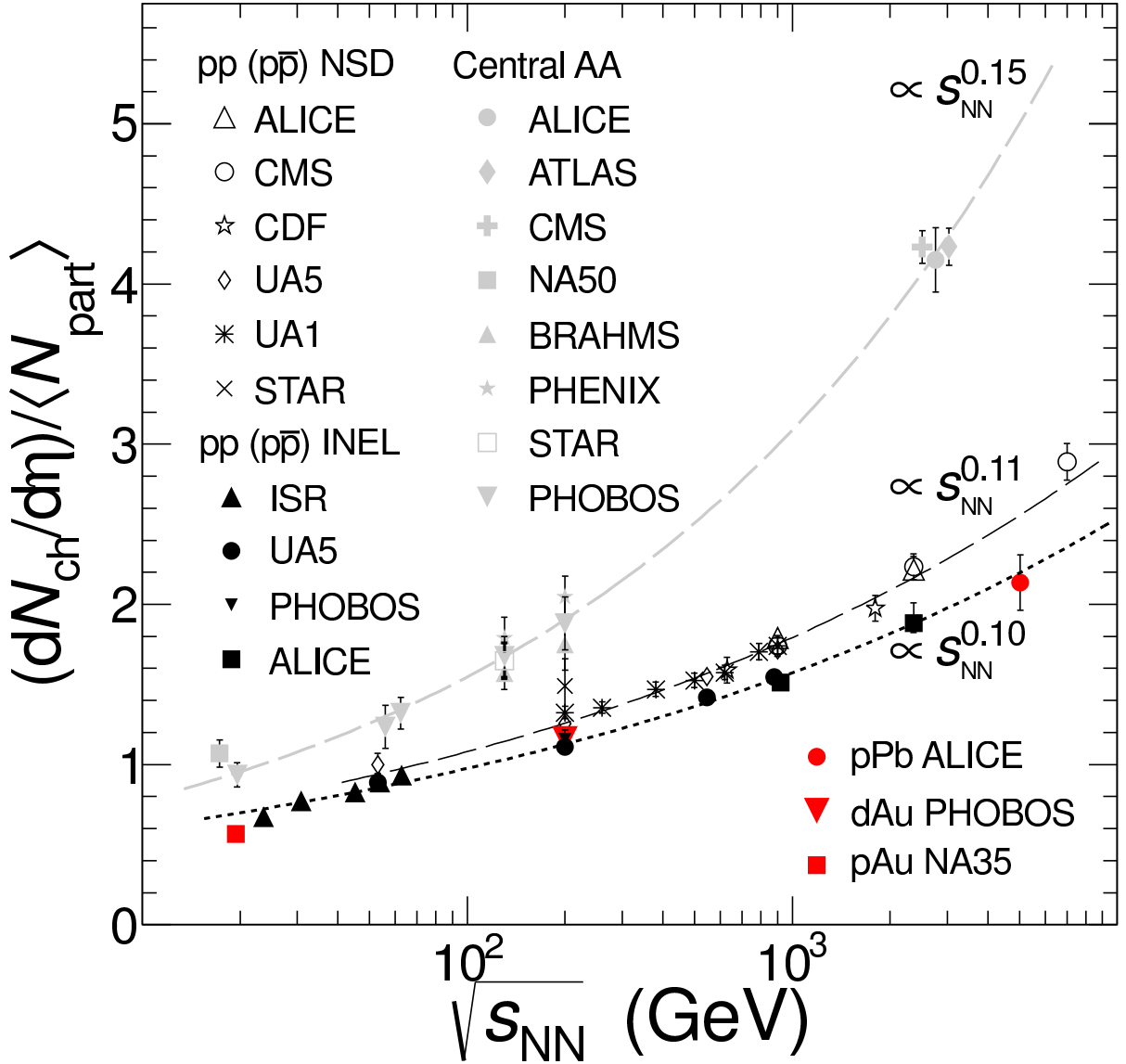


Fig. 2: Charged-particle pseudorapidity density at midrapidity normalized to the number of participants, calculated with the Glauber model, for p–Pb, p–Au and d–Au [8, 9] collisions as a function of $\sqrt{s_{NN}}$, compared to NSD [10–16], and inelastic [17–20] pp (p \bar{p}) collisions, as well as central heavy-ion [20–31] collisions. The curves $\propto s_{NN}^{0.11}$ and $s_{NN}^{0.15}$ (from [29]) are superimposed on the NSD pp (p \bar{p}) and central heavy-ion data, respectively, while $\propto s_{NN}^{0.10}$ (from [19]) on the inelastic pp (p \bar{p}) data.

radius of 6.62 ± 0.06 fm and a skin depth of 0.546 ± 0.010 fm, a hard-sphere exclusion distance of 0.4 ± 0.4 fm for the lead nucleus, a radius of 0.6 ± 0.2 fm for the proton, and an inelastic nucleon–nucleon cross section of 70 ± 5 mb. The latter is obtained by interpolating data at different centre-of-mass energies [41] including measurements at 2.76 and 7 TeV [34, 42]. The number of participants for minimum-bias events is found to be distributed with an average $\langle N_{part} \rangle = 7.9 \pm 0.6$ and an r.m.s. width of 5.1. The uncertainty of 7.6% on $\langle N_{part} \rangle$ is obtained by varying the parameters of the Glauber calculation within the ranges mentioned above (as explained in Ref. [43]). Note that the number of participants would increase by only 2.5% if normalized to NSD events in the Glauber calculation. Normalizing to the number of participants gives $\langle dN_{ch}/d\eta_{cms} \rangle / \langle N_{part} \rangle = 2.14 \pm 0.17$ (syst.). In Fig. 2, this value is compared to measurements in p–Au and d–Au [8, 9] collisions, NSD [10–16], and inelastic [17–20]

pp ($p\bar{p}$), as well as central heavy-ion [20–31] collisions, over a wide range of collision energies. (Data for d–Au at $\sqrt{s_{NN}} = 200$ GeV from [44, 45] are consistent with that from [9] and not shown in the figure.) The $(dN_{ch}/d\eta_{cms})/\langle N_{part} \rangle$ at $\sqrt{s_{NN}} = 5.02$ TeV is found to be 16% lower than in NSD pp and consistent with inelastic pp collisions interpolated to $\sqrt{s_{NN}} = 5.02$ TeV, and 84% higher than in d–Au collisions at $\sqrt{s_{NN}} = 0.2$ TeV.

In summary, the charged-particle pseudorapidity density in $|\eta_{lab}| < 2$ in non-single-diffractive p–Pb collisions at $\sqrt{s_{NN}} = 5.02$ TeV is presented. At midrapidity, $dN_{ch}/d\eta_{cms} = 16.81 \pm 0.71$ (*syst.*) is measured, corresponding to 2.14 ± 0.17 (*syst.*) charged particles per unit pseudorapidity per participant, where the number of participants are calculated with the Glauber model. The new measurement extends the study of charged-particle densities in proton–nucleus collisions into the TeV scale, and provides new constraints on the description of particle production in high-energy nuclear collisions.

Acknowledgements

The ALICE collaboration would like to thank J. Albacete, A. Dumitru, M. Gyulassy, A. Rezaeian, V. Topor, P. Tribedy and X.-N. Wang for helpful discussions and their model predictions.

The ALICE collaboration would like to thank all its engineers and technicians for their invaluable contributions to the construction of the experiment and the CERN accelerator teams for the outstanding performance of the LHC complex.

The ALICE collaboration acknowledges the following funding agencies for their support in building and running the ALICE detector:

State Committee of Science, Calouste Gulbenkian Foundation from Lisbon and Swiss Fonds Kidagan, Armenia;

Conselho Nacional de Desenvolvimento Científico e Tecnológico (CNPq), Financiadora de Estudos e Projetos (FINEP), Fundação de Amparo à Pesquisa do Estado de São Paulo (FAPESP);

National Natural Science Foundation of China (NSFC), the Chinese Ministry of Education (CMOE) and the Ministry of Science and Technology of China (MSTC);

Ministry of Education and Youth of the Czech Republic;

Danish Natural Science Research Council, the Carlsberg Foundation and the Danish National Research Foundation;

The European Research Council under the European Community’s Seventh Framework Programme; Helsinki Institute of Physics and the Academy of Finland;

French CNRS-IN2P3, the ‘Region Pays de Loire’, ‘Region Alsace’, ‘Region Auvergne’ and CEA, France;

German BMBF and the Helmholtz Association;

General Secretariat for Research and Technology, Ministry of Development, Greece;

Hungarian OTKA and National Office for Research and Technology (NKTH);

Department of Atomic Energy and Department of Science and Technology of the Government of India;

Istituto Nazionale di Fisica Nucleare (INFN) of Italy;

MEXT Grant-in-Aid for Specially Promoted Research, Japan;

Joint Institute for Nuclear Research, Dubna;

National Research Foundation of Korea (NRF);

CONACYT, DGAPA, México, ALFA-EC and the HELEN Program (High-Energy physics Latin-American–European Network);

Stichting voor Fundamenteel Onderzoek der Materie (FOM) and the Nederlandse Organisatie voor Wetenschappelijk Onderzoek (NWO), Netherlands;

Research Council of Norway (NFR);

Polish Ministry of Science and Higher Education;

National Authority for Scientific Research - NASR (Autoritatea Națională pentru Cercetare Științifică -

ANCS);

Ministry of Education and Science of Russian Federation, International Science and Technology Center, Russian Academy of Sciences, Russian Federal Agency of Atomic Energy, Russian Federal Agency for Science and Innovations and CERN-INTAS;

Ministry of Education of Slovakia;

Department of Science and Technology, South Africa;

CIEMAT, EELA, Ministerio de Educación y Ciencia of Spain, Xunta de Galicia (Consellería de Educación), CEADEN, Cubaenergía, Cuba, and IAEA (International Atomic Energy Agency);

Swedish Research Council (VR) and Knut & Alice Wallenberg Foundation (KAW);

Ukraine Ministry of Education and Science;

United Kingdom Science and Technology Facilities Council (STFC);

The United States Department of Energy, the United States National Science Foundation, the State of Texas, and the State of Ohio.

References

- [1] C. Salgado, J. Alvarez-Muniz, F. Arleo, N. Armesto, M. Botje, *et al.*, “Proton-Nucleus Collisions at the LHC: Scientific Opportunities and Requirements,” *J.Phys.G* **G39** (2012) 015010, arXiv:1105.3919 [hep-ph].
- [2] ALICE Collaboration, K. Aamodt *et al.*, “The ALICE experiment at the CERN LHC,” *JINST* **3** (2008) S08002.
- [3] A. Dumitru, D. E. Kharzeev, E. M. Levin, and Y. Nara, “Gluon Saturation in pA Collisions at the LHC: KLN Model Predictions For Hadron Multiplicities,” *Phys.Rev.* **C85** (2012) 044920, arXiv:1111.3031 [hep-ph].
- [4] G. Barnafoldi, J. Barrette, M. Gyulassy, P. Levai, and V. Topor Pop, “Predictions for p+Pb at 4.4A TeV to Test Initial State Nuclear Shadowing at energies available at the CERN Large Hadron Collider,” *Phys.Rev.* **C85** (2012) 024903, arXiv:1111.3646 [nucl-th].
- [5] P. Tribedy and R. Venugopalan, “QCD saturation at the LHC: comparisons of models to p+p and A+A data and predictions for p+Pb collisions,” *Phys.Lett.* **B710** (2012) 125–133, arXiv:1112.2445 [hep-ph].
- [6] R. Xu, W.-T. Deng, and X.-N. Wang, “Nuclear modification of high- p_T hadron spectra in p+A collisions at LHC,” arXiv:1204.1998 [nucl-th].
- [7] J. L. Albacete, A. Dumitru, H. Fujii, and Y. Nara, “CGC predictions for p+Pb collisions at the LHC,” arXiv:1209.2001 [hep-ph].
- [8] NA35 Collaboration, T. Alber *et al.*, “Charged particle production in proton, deuteron, oxygen and sulphur nucleus collisions at 200-GeV per nucleon,” *Eur.Phys.J.* **C2** (1998) 643–659, arXiv:hep-ex/9711001 [hep-ex]. The reported value has been obtained by multiplying the quoted results for negative charged hadrons by 2, and using HIJING [40] a correction for -20% with a $\pm 10\%$ uncertainty has been applied for the transformation from rapidity to pseudorapidity.
- [9] PHOBOS Collaboration, B. Back *et al.*, “Pseudorapidity distribution of charged particles in d + Au collisions at $\sqrt{s_{NN}} = 200$ GeV,” *Phys.Rev.Lett.* **93** (2004) 082301, arXiv:nucl-ex/0311009 [nucl-ex].
- [10] UA1 Collaboration, C. Albajar *et al.*, “A Study of the General Characteristics of $p\bar{p}$ Collisions at $\sqrt{s} = 0.2$ -TeV to 0.9-TeV,” *Nucl.Phys.* **B335** (1990) 261.

- [11] **UA5 Collaboration** Collaboration, K. Alpgard *et al.*, “Particle Multiplicities in anti-p p Interactions at $s^{*(1/2)} = 540\text{-GeV}$,” *Phys.Lett.* **B121** (1983) 209.
- [12] **UA5 Collaboration** Collaboration, G. Alner *et al.*, “Scaling of Pseudorapidity Distributions at c.m. Energies Up to 0.9-TeV,” *Z.Phys.* **C33** (1986) 1–6.
- [13] **STAR Collaboration**, B. I. Abelev *et al.*, “Systematic measurements of identified particle spectra in pp, d + Au, and Au + Au collisions at the star detector,” *Phys. Rev. C* **79** (Mar, 2009) 034909. <http://link.aps.org/doi/10.1103/PhysRevC.79.034909>.
- [14] **CDF Collaboration** Collaboration, F. Abe *et al.*, “Pseudorapidity distributions of charged particles produced in $\bar{p}p$ interactions at $\sqrt{s} = 630\text{ GeV}$ and 1800 GeV ,” *Phys.Rev.* **D41** (1990) 2330.
- [15] **ALICE Collaboration** Collaboration, K. Aamodt *et al.*, “Charged-particle multiplicity measurement in proton-proton collisions at $\sqrt{s} = 7\text{ TeV}$ with ALICE at LHC,” *Eur.Phys.J.* **C68** (2010) 345–354, [arXiv:1004.3514](https://arxiv.org/abs/1004.3514) [hep-ex].
- [16] **CMS Collaboration**, V. Khachatryan *et al.*, “Transverse momentum and pseudorapidity distributions of charged hadrons in pp collisions at $\sqrt{s_{NN}} = 0.9$ and 2.36 TeV ,” *JHEP* **02** (2010) 041, [arXiv:1002.0621](https://arxiv.org/abs/1002.0621) [hep-ex].
- [17] W. Thome *et al.*, “Charged Particle Multiplicity Distributions in p p Collisions at ISR Energies,” *Nucl.Phys.* **B129** (1977) 365.
- [18] **UA5 Collaboration**, G. Alner *et al.*, “Scaling of Pseudorapidity Distributions at c.m. Energies Up to 0.9-TeV,” *Z.Phys.* **C33** (1986) 1–6.
- [19] **ALICE Collaboration**, K. Aamodt *et al.*, “Charged-particle multiplicity measurement in proton-proton collisions at $\sqrt{s} = 0.9$ and 2.36 TeV with ALICE at LHC,” *Eur.Phys.J.* **C68** (2010) 89–108, [arXiv:1004.3034](https://arxiv.org/abs/1004.3034) [hep-ex].
- [20] **PHOBOS Collaboration**, B. Alver *et al.*, “Phobos results on charged particle multiplicity and pseudorapidity distributions in Au+Au, Cu+Cu, d+Au, and p+p collisions at ultra-relativistic energies,” *Phys.Rev.* **C83** (2011) 024913, [arXiv:1011.1940](https://arxiv.org/abs/1011.1940) [nucl-ex].
- [21] **NA50 Collaboration**, M. C. Abreu *et al.*, “Scaling of charged particle multiplicity in Pb + Pb collisions at SPS energies,” *Phys. Lett.* **B530** (2002) 43–55.
- [22] **STAR Collaboration**, C. Adler *et al.*, “Multiplicity distribution and spectra of negatively charged hadrons in Au + Au collisions at $\sqrt{s_{NN}} = 130\text{ GeV}$,” *Phys. Rev. Lett.* **87** (2001) 112303, [arXiv:nuc1-ex/0106004](https://arxiv.org/abs/nuc1-ex/0106004).
- [23] **BRAHMS Collaboration**, I. G. Bearden *et al.*, “Charged particle densities from Au + Au collisions at $\sqrt{s_{NN}} = 130\text{ GeV}$,” *Phys. Lett.* **B523** (2001) 227–233, [arXiv:nuc1-ex/0108016](https://arxiv.org/abs/nuc1-ex/0108016).
- [24] **BRAHMS Collaboration**, I. G. Bearden *et al.*, “Pseudorapidity distributions of charged particles from Au+Au collisions at the maximum RHIC energy,” *Phys. Rev. Lett.* **88** (2002) 202301, [arXiv:nuc1-ex/0112001](https://arxiv.org/abs/nuc1-ex/0112001).
- [25] **PHENIX Collaboration**, K. Adcox *et al.*, “Centrality dependence of charged particle multiplicity in Au Au collisions at $\sqrt{s_{NN}} = 130\text{ GeV}$,” *Phys. Rev. Lett.* **86** (2001) 3500–3505, [arXiv:nuc1-ex/0012008](https://arxiv.org/abs/nuc1-ex/0012008).

- [26] **PHOBOS** Collaboration, B. B. Back *et al.*, “Charged particle multiplicity near mid-rapidity in central Au + Au collisions at $S^{(1/2)} = 56$ -A/GeV and 130- A/GeV,” *Phys. Rev. Lett.* **85** (2000) 3100–3104, arXiv:hep-ex/0007036.
- [27] **PHOBOS** Collaboration, B. B. Back *et al.*, “Charged particle pseudorapidity density distributions from Au+Au collisions at $\sqrt{s_{NN}} = 130$ GeV,” *Phys. Rev. Lett.* **87** (2001) 102303, arXiv:nucl-ex/0106006.
- [28] B. B. Back *et al.*, “The significance of the fragmentation region in ultrarelativistic heavy ion collisions,” *Phys. Rev. Lett.* **91** (2003) 052303, arXiv:nucl-ex/0210015.
- [29] **ALICE** Collaboration, B. Abelev *et al.*, “Charged-particle multiplicity density at mid-rapidity in central Pb-Pb collisions at $\sqrt{s_{NN}} = 2.76$ TeV,” *Phys.Rev.Lett.* **105** (2010) 252301, arXiv:1011.3916 [nucl-ex].
- [30] **ATLAS** Collaboration, G. Aad *et al.*, “Measurement of the centrality dependence of the charged particle pseudorapidity distribution in lead-lead collisions at $\sqrt{s_{NN}} = 2.76$ TeV with the ATLAS detector,” *Phys.Lett.* **B710** (2012) 363–382, arXiv:1108.6027 [hep-ex].
- [31] **CMS** Collaboration, S. Chatrchyan *et al.*, “Dependence on pseudorapidity and centrality of charged hadron production in PbPb collisions at a nucleon-nucleon centre-of-mass energy of 2.76 TeV,” *JHEP* **1108** (2011) 141, arXiv:1107.4800 [nucl-ex].
- [32] S. Roesler, R. Engel, and J. Ranft, “The Monte Carlo event generator DPMJET-III,” arXiv:hep-ph/0012252.
- [33] R. Engel, J. Ranft, and S. Roesler, “Hard diffraction in hadron hadron interactions and in photoproduction,” *Phys.Rev.* **D52** (1995) 1459–1468, arXiv:hep-ph/9502319 [hep-ph].
- [34] **ALICE** Collaboration, B. Abelev *et al.*, “Measurement of inelastic, single- and double-diffraction cross sections in proton–proton collisions at the LHC with ALICE,” arXiv:1208.4968 [hep-ex].
- [35] B. Alver, M. Baker, C. Loizides, and P. Steinberg, “The PHOBOS Glauber Monte Carlo,” arXiv:0805.4411 [nucl-ex].
- [36] O. Djuvsland and J. Nystrand, “Single and Double Photonuclear Excitations in Pb+Pb Collisions at $\sqrt{s_{NN}} = 2.76$ TeV at the CERN Large Hadron Collider,” *Phys.Rev.* **C83** (2011) 041901, arXiv:1011.4908 [hep-ph].
- [37] T. Sjostrand, S. Mrenna, and P. Z. Skands, “PYTHIA 6.4 Physics and Manual,” *JHEP* **0605** (2006) 026, arXiv:hep-ph/0603175 [hep-ph].
- [38] R. Brun *et al.* *CERN Program Library Long Write-up, W5013, GEANT Detector Description and Simulation Tool* (1994).
- [39] V. Andersen *et al.*, “The fluka code for space applications: recent developments,” *Advances in Space Research* **34** no. 6, (2004) 1302 – 1310.
<http://www.sciencedirect.com/science/article/pii/S0273117704002054>.
- [40] X.-N. Wang and M. Gyulassy, “Hijing: A monte carlo model for multiple jet production in p p, p a and a a collisions,” *Phys. Rev. D* **44** (1991) 3501.
- [41] **Particle Data Group** Collaboration, K. Nakamura *et al.*, “Review of particle physics,” *J. Phys.* **G37** (2010) 075021.

- [42] **TOTEM** Collaboration, G. Antchev, P. Aspell, I. Atanassov, V. Avati, J. Baechler, *et al.*, “First measurement of the total proton-proton cross section at the LHC energy of $\sqrt{s} = 7$ TeV,” *Europhys.Lett.* **96** (2011) 21002, arXiv:1110.1395 [hep-ex].
- [43] **ALICE** Collaboration, K. Aamodt *et al.*, “Centrality dependence of the charged-particle multiplicity density at mid-rapidity in Pb-Pb collisions at $\sqrt{s_{NN}} = 2.76$ TeV,” *Phys.Rev.Lett.* **106** (2011) 032301, arXiv:1012.1657 [nucl-ex].
- [44] **BRAHMS** Collaboration, I. Arsene *et al.*, “Centrality dependence of charged particle pseudorapidity distributions from d+Au collisions at $\sqrt{s_{NN}} = 200$ GeV,” *Phys.Rev.Lett.* **94** (2005) 032301, arXiv:nucl-ex/0401025 [nucl-ex].
- [45] **STAR** Collaboration, B. Abelev *et al.*, “Charged particle distributions and nuclear modification at high rapidities in d + Au collisions at $\sqrt{s_{NN}} = 200$ GeV,” arXiv:nucl-ex/0703016 [nucl-ex].

A The ALICE Collaboration

B. Abelev⁷², J. Adam³⁷, D. Adamová⁷⁸, A.M. Adare¹²⁴, M.M. Aggarwal⁸², G. Aglieri Rinella³³, M. Agnello¹⁰¹, A.G. Agocs⁶⁴, A. Agostinelli²³, Z. Ahammed¹²⁰, N. Ahmad¹⁷, A. Ahmad Masoodi¹⁷, S.U. Ahn^{40,66}, S.A. Ahn⁶⁶, M. Ajaz¹⁵, A. Akimov⁵⁰, D. Aleksandrov⁹³, B. Alessandro¹⁰¹, R. Alfaro Molina⁶⁰, A. Alici^{97,12}, A. Alkin³, E. Almaráz Aviña⁶⁰, J. Alme³⁵, T. Alt³⁹, V. Altini³¹, S. Altinpinar¹⁸, I. Altsybeev¹²¹, C. Andrei⁷⁵, A. Andronic⁹⁰, V. Anguelov⁸⁷, J. Anielski⁵⁸, C. Anson¹⁹, T. Antičić⁹¹, F. Antinori⁹⁹, P. Antonioli⁹⁷, L. Aphecetche¹⁰⁶, H. Appelshäuser⁵⁶, N. Arbor⁶⁸, S. Arcelli²³, A. Arend⁵⁶, N. Armesto¹⁶, R. Arnaldi¹⁰¹, T. Aronsson¹²⁴, I.C. Arsene⁹⁰, M. Arslanok⁵⁶, A. Asryan¹²¹, A. Augustinus³³, R. Averbeck⁹⁰, T.C. Awes⁷⁹, J. Äystö⁴², M.D. Azmi^{17,84}, M. Bach³⁹, A. Badalà⁹⁸, Y.W. Baek^{67,40}, R. Bailhache⁵⁶, R. Bala^{85,101}, R. Baldini Ferroli¹², A. Baldisseri¹⁴, F. Baltasar Dos Santos Pedrosa³³, J. Bán⁵¹, R.C. Baral⁵², R. Barbera²⁷, F. Barile³¹, G.G. Barnaföldi⁶⁴, L.S. Barnby⁹⁵, V. Barret⁶⁷, J. Bartke¹⁰⁸, M. Basile²³, N. Bastid⁶⁷, S. Basu¹²⁰, B. Bathen⁵⁸, G. Batigne¹⁰⁶, B. Batyunya⁶³, C. Baumann⁵⁶, I.G. Bearden⁷⁶, H. Beck⁵⁶, N.K. Behera⁴⁴, I. Belikov⁶², F. Bellini²³, R. Bellwied¹¹⁴, E. Belmont-Moreno⁶⁰, G. Bencedi⁶⁴, S. Beole²², I. Berceau⁷⁵, A. Bercuci⁷⁵, Y. Berdnikov⁸⁰, D. Berenyi⁶⁴, A.A.E. Bergognon¹⁰⁶, D. Berzano^{22,101}, L. Betev³³, A. Bhasin⁸⁵, A.K. Bhati⁸², J. Bhom¹¹⁸, L. Bianchi²², N. Bianchi⁶⁹, J. Bielčák³⁷, J. Bielčáková⁷⁸, A. Bilandžić⁷⁶, S. Bjelogrić⁴⁹, F. Blanco¹¹⁴, F. Blanco¹⁰, D. Blau⁹³, C. Blume⁵⁶, M. Boccioni³³, S. Böttger⁵⁵, A. Bogdanov⁷³, H. Bøggild⁷⁶, M. Bogolyubsky⁴⁷, L. Boldizsár⁶⁴, M. Bombara³⁸, J. Book⁵⁶, H. Borel¹⁴, A. Borissov¹²³, F. Bossú⁸⁴, M. Botje⁷⁷, E. Botta²², E. Braidot⁷¹, P. Braun-Munzinger⁹⁰, M. Bregant¹⁰⁶, T. Breitner⁵⁵, T.A. Browning⁸⁸, M. Broz³⁶, R. Brun³³, E. Bruna^{22,101}, G.E. Bruno³¹, D. Budnikov⁹², H. Buesching⁵⁶, S. Bufalino^{22,101}, O. Busch⁸⁷, Z. Buthelezi⁸⁴, D. Caballero Orduna¹²⁴, D. Caffarri^{28,99}, X. Cai⁷, H. Caines¹²⁴, E. Calvo Villar⁹⁶, P. Camerini²⁵, V. Canoa Roman¹¹, G. Cara Romeo⁹⁷, W. Carena³³, F. Carena³³, N. Carlin Filho¹¹¹, F. Carminati³³, A. Casanova Díaz⁶⁹, J. Castillo Castellanos¹⁴, J.F. Castillo Hernandez⁹⁰, E.A.R. Casula²⁴, V. Catanescu³³, C. Cavicchioli³³, C. Ceballos Sanchez⁹, J. Cepila³⁷, P. Cerello¹⁰¹, B. Chang^{42,126}, S. Chapeland³³, J.L. Charvet¹⁴, S. Chattopadhyay¹²⁰, S. Chattopadhyay⁹⁴, I. Chawla⁸², M. Cherney⁸¹, C. Cheshkov^{33,113}, B. Cheynis¹¹³, V. Chibante Barroso³³, D.D. Chinellato¹¹⁴, P. Chochula³³, M. Chojnacki^{76,49}, S. Choudhury¹²⁰, P. Christakoglou⁷⁷, C.H. Christensen⁷⁶, P. Christiansen³², T. Chujo¹¹⁸, S.U. Chung⁸⁹, C. Cicalo¹⁰⁰, L. Cifarelli^{23,33,12}, F. Cindolo⁹⁷, J. Cleymans⁸⁴, F. Coccetti¹², F. Colamaria³¹, D. Colella³¹, A. Collu²⁴, G. Conesa Balbastre⁶⁸, Z. Conesa del Valle³³, M.E. Connors¹²⁴, G. Contin²⁵, J.G. Contreras¹¹, T.M. Cormier¹²³, Y. Corrales Morales²², P. Cortese³⁰, I. Cortés Maldonado², M.R. Cosentino⁷¹, F. Costa³³, M.E. Cotallo¹⁰, E. Crescio¹¹, P. Crochet⁶⁷, E. Cruz Alaniz⁶⁰, E. Cuautle⁵⁹, L. Cunqueiro⁶⁹, A. Dainese^{28,99}, H.H. Dalsgaard⁷⁶, A. Danu⁵⁴, K. Das⁹⁴, I. Das⁴⁶, S. Das⁴, D. Das⁹⁴, S. Dash⁴⁴, A. Dash¹¹², S. De¹²⁰, G.O.V. de Barros¹¹¹, A. De Caro^{29,12}, G. de Cataldo¹⁰⁴, J. de Cuveland³⁹, A. De Falco²⁴, D. De Gruttola²⁹, H. Delagrange¹⁰⁶, A. Deloff⁷⁴, N. De Marco¹⁰¹, E. Dénes⁶⁴, S. De Pasquale²⁹, A. Deppman¹¹¹, G. D'Erasmus³¹, R. de Rooij⁴⁹, M.A. Diaz Corchero¹⁰, D. Di Bari³¹, T. Dietel⁵⁸, C. Di Giglio³¹, S. Di Liberto¹⁰³, A. Di Mauro³³, P. Di Nezza⁶⁹, R. Divià³³, Ø. Djuvsland¹⁸, A. Dobrin^{123,32}, T. Dobrowolski⁷⁴, B. Dönigus⁹⁰, O. Dordic²¹, O. Driga¹⁰⁶, A.K. Dubey¹²⁰, A. Dubla⁴⁹, L. Ducroux¹¹³, P. Dupieux⁶⁷, M.R. Dutta Majumdar¹²⁰, A.K. Dutta Majumdar⁹⁴, D. Elia¹⁰⁴, D. Emschermann⁵⁸, H. Engel⁵⁵, B. Erazmus^{33,106}, H.A. Erdal³⁵, B. Espagnon⁴⁶, M. Estienne¹⁰⁶, S. Esumi¹¹⁸, D. Evans⁹⁵, G. Eyyubova²¹, D. Fabris^{28,99}, J. Faivre⁶⁸, D. Falchieri²³, A. Fantoni⁶⁹, M. Fasel⁹⁰, R. Fearick⁸⁴, D. Fehler¹⁸, L. Feldkamp⁵⁸, D. Felea⁵⁴, A. Feliciello¹⁰¹, B. Fenton-Olsen⁷¹, G. Feofilov¹²¹, A. Fernández Téllez², A. Ferretti²², A. Festanti²⁸, J. Figiel¹⁰⁸, M.A.S. Figueredo¹¹¹, S. Filchagin⁹², D. Finogeev⁴⁸, F.M. Fionda³¹, E.M. Fiore³¹, M. Floris³³, S. Foertsch⁸⁴, P. Foka⁹⁰, S. Fokin⁹³, E. Fragiaco¹⁰², A. Francescon^{33,28}, U. Frankenfeld⁹⁰, U. Fuchs³³, C. Furget⁶⁸, M. Fusco Girard²⁹, J.J. Gaardhøje⁷⁶, M. Gagliardi²², A. Gago⁹⁶, M. Gallio²², D.R. Gangadharan¹⁹, P. Ganoti⁷⁹, C. Garabatos⁹⁰, E. Garcia-Solis¹³, I. Garishvili⁷², J. Gerhard³⁹, M. Germain¹⁰⁶, C. Geuna¹⁴, A. Gheata³³, M. Gheata^{54,33}, B. Ghidini³¹, P. Ghosh¹²⁰, P. Gianotti⁶⁹, M.R. Girard¹²², P. Giubellino³³, E. Gladysz-Dziadus¹⁰⁸, P. Glässel⁸⁷, R. Gomez^{110,11}, E.G. Ferreira¹⁶, L.H. González-Trueba⁶⁰, P. González-Zamora¹⁰, S. Gorbunov³⁹, A. Goswami⁸⁶, S. Gotovac¹⁰⁷, V. Grabski⁶⁰, L.K. Graczykowski¹²², R. Grajcarek⁸⁷, A. Grelli⁴⁹, A. Grigoras³³, C. Grigoras³³, V. Grigoriev⁷³, S. Grigoryan⁶³, A. Grigoryan¹, B. Grinyov³, N. Grión¹⁰², P. Gros³², J.F. Grosse-Oetringhaus³³, J.-Y. Grossiord¹¹³, R. Grosso³³, F. Guber⁴⁸, R. Guernane⁶⁸, C. Guerra Gutierrez⁹⁶, B. Guerzoni²³, M. Guilbaud¹¹³, K. Gulbrandsen⁷⁶, H. Gulkanyan¹, T. Gunji¹¹⁷, A. Gupta⁸⁵, R. Gupta⁸⁵, Ø. Haaland¹⁸, C. Hadjidakis⁴⁶, M. Haiduc⁵⁴, H. Hamagaki¹¹⁷, G. Hamar⁶⁴, B.H. Han²⁰, L.D. Hanratty⁹⁵, A. Hansen⁷⁶, Z. Harmanová-Tóthová³⁸, J.W. Harris¹²⁴, M. Hartig⁵⁶, A. Harton¹³, D. Hasegan⁵⁴, D. Hatzifotiadou⁹⁷, S. Hayashi¹¹⁷, A. Hayrapetyan^{33,1}, S.T. Heckel⁵⁶, M. Heide⁵⁸, H. Helstrup³⁵, A. Hergelegiu⁷⁵, G. Herrera Corral¹¹, N. Herrmann⁸⁷, B.A. Hess¹¹⁹,

K.F. Hetland³⁵, B. Hicks¹²⁴, B. Hippolyte⁶², Y. Hori¹¹⁷, P. Hristov³³, I. Hřivnáčová⁴⁶, M. Huang¹⁸,
 T.J. Humanic¹⁹, D.S. Hwang²⁰, R. Ichou⁶⁷, R. Ilkaev⁹², I. Ilkiv⁷⁴, M. Inaba¹¹⁸, E. Incani²⁴, G.M. Innocenti²²,
 P.G. Innocenti³³, M. Ippolitov⁹³, M. Irfan¹⁷, C. Ivan⁹⁰, V. Ivanov⁸⁰, A. Ivanov¹²¹, M. Ivanov⁹⁰,
 O. Ivanytskyi³, A. Jachořkowski²⁷, P. M. Jacobs⁷¹, H.J. Jang⁶⁶, R. Janik³⁶, M.A. Janik¹²²,
 P.H.S.Y. Jayarathna¹¹⁴, S. Jena⁴⁴, D.M. Jha¹²³, R.T. Jimenez Bustamante⁵⁹, P.G. Jones⁹⁵, H. Jung⁴⁰,
 A. Jusko⁹⁵, A.B. Kaidalov⁵⁰, S. Kalcher³⁹, P. Kaliňák⁵¹, T. Kalliokoski⁴², A. Kalweit^{57,33}, J.H. Kang¹²⁶,
 V. Kaplin⁷³, A. Karasu Uysal^{33,125}, O. Karavichev⁴⁸, T. Karavicheva⁴⁸, E. Karpechev⁴⁸, A. Kazantsev⁹³,
 U. Keschull⁵⁵, R. Keidel¹²⁷, K. H. Khan¹⁵, P. Khan⁹⁴, M.M. Khan¹⁷, S.A. Khan¹²⁰, A. Khanzadeev⁸⁰,
 Y. Kharlov⁴⁷, B. Kileng³⁵, D.W. Kim^{40,66}, T. Kim¹²⁶, B. Kim¹²⁶, J.H. Kim²⁰, J.S. Kim⁴⁰, M. Kim⁴⁰,
 M. Kim¹²⁶, S. Kim²⁰, D.J. Kim⁴², S. Kirsch³⁹, I. Kisel³⁹, S. Kiselev⁵⁰, A. Kisiel¹²², J.L. Klay⁶, J. Klein⁸⁷,
 C. Klein-Bösing⁵⁸, M. Kliemant⁵⁶, A. Kluge³³, M.L. Knichel⁹⁰, A.G. Knospe¹⁰⁹, M.K. Köhler⁹⁰,
 T. Kollegger³⁹, A. Kolojvari¹²¹, V. Kondratiev¹²¹, N. Kondratyeva⁷³, A. Konevskikh⁴⁸, R. Kour⁹⁵,
 V. Kovalenko¹²¹, M. Kowalski¹⁰⁸, S. Kox⁶⁸, G. Koyithatta Meethalevedu⁴⁴, J. Kral⁴², I. Králik⁵¹,
 F. Kramer⁵⁶, A. Kravčáková³⁸, T. Krawutschke^{87,34}, M. Krelina³⁷, M. Kretz³⁹, M. Krivda^{95,51}, F. Krizek⁴²,
 M. Krus³⁷, E. Kryshen⁸⁰, M. Krzewicki⁹⁰, Y. Kucheriaev⁹³, T. Kugathanan³³, C. Kuhn⁶², P.G. Kuijjer⁷⁷,
 I. Kulakov⁵⁶, J. Kumar⁴⁴, P. Kurashvili⁷⁴, A. Kurepin⁴⁸, A.B. Kurepin⁴⁸, A. Kuryakin⁹², V. Kuschpil⁷⁸,
 S. Kuschpil⁷⁸, H. Kvaerno²¹, M.J. Kweon⁸⁷, Y. Kwon¹²⁶, P. Ladrón de Guevara⁵⁹, I. Lakomov⁴⁶, R. Langoy¹⁸,
 S.L. La Pointe⁴⁹, C. Lara⁵⁵, A. Lardeux¹⁰⁶, P. La Rocca²⁷, R. Lea²⁵, M. Lechman³³, K.S. Lee⁴⁰, S.C. Lee⁴⁰,
 G.R. Lee⁹⁵, I. Legrand³³, J. Lehnert⁵⁶, M. Lenhardt⁹⁰, V. Lenti¹⁰⁴, H. León⁶⁰, M. Leoncino¹⁰¹,
 I. León Monzón¹¹⁰, H. León Vargas⁵⁶, P. Lévai⁶⁴, J. Lien¹⁸, R. Lietava⁹⁵, S. Lindal²¹, V. Lindenstruth³⁹,
 C. Lippmann^{90,33}, M.A. Lisa¹⁹, H.M. Ljunggren³², P.I. Loenne¹⁸, V.R. Loggins¹²³, V. Loginov⁷³,
 D. Lohner⁸⁷, C. Loizides⁷¹, K.K. Loo⁴², X. Lopez⁶⁷, E. López Torres⁹, G. Løvhøiden²¹, X.-G. Lu⁸⁷,
 P. Luetig⁵⁶, M. Lunardon²⁸, J. Luo⁷, G. Luparello⁴⁹, C. Luzzi³³, K. Ma⁷, R. Ma¹²⁴,
 D.M. Madagodahettige-Don¹¹⁴, A. Maevskaya⁴⁸, M. Mager^{57,33}, D.P. Mahapatra⁵², A. Maire⁸⁷, M. Malaev⁸⁰,
 I. Maldonado Cervantes⁵⁹, L. Malinina^{63,ii}, D. Mal'Kevich⁵⁰, P. Malzacher⁹⁰, A. Mamonov⁹², L. Manceau¹⁰¹,
 L. Mangotra⁸⁵, V. Manko⁹³, F. Manso⁶⁷, V. Manzari¹⁰⁴, Y. Mao⁷, M. Marchisone^{67,22}, J. Mareš⁵³,
 G.V. Margagliotti^{25,102}, A. Margotti⁹⁷, A. Marín⁹⁰, C. Markert¹⁰⁹, M. Marquard⁵⁶, I. Martashvili¹¹⁶,
 N.A. Martin⁹⁰, P. Martinengo³³, M.I. Martínez², A. Martínez Davalos⁶⁰, G. Martínez García¹⁰⁶, Y. Martynov³,
 A. Mas¹⁰⁶, S. Masciocchi⁹⁰, M. Maserà²², A. Masoni¹⁰⁰, L. Massacrier¹⁰⁶, A. Mastroserio³¹,
 Z.L. Matthews⁹⁵, A. Matyja^{108,106}, C. Mayer¹⁰⁸, J. Mazer¹¹⁶, M.A. Mazzoni¹⁰³, F. Meddi²⁶,
 A. Menchaca-Rocha⁶⁰, J. Mercado Pérez⁸⁷, M. Meres³⁶, Y. Miake¹¹⁸, L. Milano²², J. Milosevic^{21,iii},
 A. Mischke⁴⁹, A.N. Mishra^{86,45}, D. Miśkowiec^{90,33}, C. Mitu⁵⁴, S. Mizuno¹¹⁸, J. Mlynarz¹²³, B. Mohanty¹²⁰,
 L. Molnar^{64,33,62}, L. Montaña Zetina¹¹, M. Monteno¹⁰¹, E. Montes¹⁰, T. Moon¹²⁶, M. Morando²⁸,
 D.A. Moreira De Godoy¹¹¹, S. Moretto²⁸, A. Morreale⁴², A. Morsch³³, V. Muccifora⁶⁹, E. Mudnic¹⁰⁷,
 S. Muhuri¹²⁰, M. Mukherjee¹²⁰, H. Müller³³, M.G. Munhoz¹¹¹, L. Musa³³, A. Musso¹⁰¹, B.K. Nandi⁴⁴,
 R. Nania⁹⁷, E. Nappi¹⁰⁴, C. Nattrass¹¹⁶, S. Navin⁹⁵, T.K. Nayak¹²⁰, S. Nazarenko⁹², A. Nedosekin⁵⁰,
 M. Nicassio^{31,90}, M. Niculescu^{54,33}, B.S. Nielsen⁷⁶, T. Niida¹¹⁸, S. Nikolaev⁹³, V. Nikolic⁹¹, V. Nikulin⁸⁰,
 S. Nikulin⁹³, B.S. Nilsen⁸¹, M.S. Nilsson²¹, F. Noferini^{97,12}, P. Nomokonov⁶³, G. Nooren⁴⁹, N. Novitzky⁴²,
 A. Nyman⁹³, A. Nyatha⁴⁴, C. Nygaard⁷⁶, J. Nystrand¹⁸, A. Ochirov¹²¹, H. Oeschler^{57,33}, S.K. Oh⁴⁰, S. Oh¹²⁴,
 J. Olińczak¹²², A.C. Oliveira Da Silva¹¹¹, C. Oppedisano¹⁰¹, A. Ortiz Velasquez^{32,59}, A. Oskarsson³²,
 P. Ostrowski¹²², J. Otwinowski⁹⁰, K. Oyama⁸⁷, K. Ozawa¹¹⁷, Y. Pachmayer⁸⁷, M. Pachr³⁷, F. Padilla²²,
 P. Pagano²⁹, G. Paic⁵⁹, F. Painke³⁹, C. Pajares¹⁶, S.K. Pal¹²⁰, A. Palaha⁹⁵, A. Palmeri⁹⁸, V. Papikyan¹,
 G.S. Pappalardo⁹⁸, W.J. Park⁹⁰, A. Passfeld⁵⁸, B. Pastirčák⁵¹, D.I. Patalakha⁴⁷, V. Paticchio¹⁰⁴, B. Paul⁹⁴,
 A. Pavlinov¹²³, T. Pawlak¹²², T. Peitzmann⁴⁹, H. Pereira Da Costa¹⁴, E. Pereira De Oliveira Filho¹¹¹,
 D. Peresunko⁹³, C.E. Pérez Lara⁷⁷, D. Perini³³, D. Perrino³¹, W. Peryt¹²², A. Pesci⁹⁷, V. Peskov^{33,59},
 Y. Pestov⁵, V. Petráček³⁷, M. Petran³⁷, M. Petris⁷⁵, P. Petrov⁹⁵, M. Petrovici⁷⁵, C. Petta²⁷, S. Piano¹⁰²,
 A. Piccotti¹⁰¹, M. Pikna³⁶, P. Pillot¹⁰⁶, O. Pinazza³³, L. Pinsky¹¹⁴, N. Pitz⁵⁶, D.B. Piyarathna¹¹⁴,
 M. Planinic⁹¹, M. Płoskoń⁷¹, J. Pluta¹²², T. Pocheptsov⁶³, S. Pochybova⁶⁴, P.L.M. Podesta-Lerma¹¹⁰,
 M.G. Poghosyan³³, K. Polák⁵³, B. Polichtchouk⁴⁷, A. Pop⁷⁵, S. Porteboeuf-Houssais⁶⁷, V. Pospíšil³⁷,
 B. Potukuchi⁸⁵, S.K. Prasad¹²³, R. Preghenella^{97,12}, F. Prino¹⁰¹, C.A. Pruneau¹²³, I. Pshenichnov⁴⁸,
 G. Puddu²⁴, V. Punin⁹², M. Putić³⁸, J. Putschke¹²³, E. Quercigh³³, H. Qvigstad²¹, A. Rachevski¹⁰²,
 A. Rademakers³³, T.S. Rähä⁴², J. Rak⁴², A. Rakotozafindrabe¹⁴, L. Ramello³⁰, A. Ramírez Reyes¹¹,
 R. Raniwala⁸⁶, S. Raniwala⁸⁶, S.S. Räsänen⁴², B.T. Rascanu⁵⁶, D. Rathee⁸², K.F. Read¹¹⁶, J.S. Real⁶⁸,
 K. Redlich^{74,61}, R.J. Reed¹²⁴, A. Rehman¹⁸, P. Reichelt⁵⁶, M. Reicher⁴⁹, R. Renfordt⁵⁶, A.R. Reolon⁶⁹,
 A. Reshetin⁴⁸, F. Rettig³⁹, J.-P. Revol³³, K. Reygers⁸⁷, L. Riccati¹⁰¹, R.A. Ricci⁷⁰, T. Richert³², M. Richerter²¹,
 P. Riedler³³, W. Riegler³³, F. Riggi^{27,98}, M. Rodríguez Cahuantzi², A. Rodríguez Manso⁷⁷, K. Røed^{18,21},

D. Rohr³⁹, D. Röhrich¹⁸, R. Romita^{90,105}, F. Ronchetti⁶⁹, P. Rosnet⁶⁷, S. Rossegger³³, A. Rossi^{33,28}, C. Roy⁶², P. Roy⁹⁴, A.J. Rubio Montero¹⁰, R. Rui²⁵, R. Russo²², E. Ryabinkin⁹³, A. Rybicki¹⁰⁸, S. Sadovsky⁴⁷, K. Šafařík³³, R. Sahoo⁴⁵, P.K. Sahu⁵², J. Saini¹²⁰, H. Sakaguchi⁴³, S. Sakai⁷¹, D. Sakata¹¹⁸, C.A. Salgado¹⁶, J. Salzwedel¹⁹, S. Sambyal⁸⁵, V. Samsonov⁸⁰, X. Sanchez Castro⁶², L. Šándor⁵¹, A. Sandoval⁶⁰, M. Sano¹¹⁸, S. Sano¹¹⁷, G. Santagati²⁷, R. Santoro^{33,12}, J. Sarkamo⁴², E. Scapparone⁹⁷, F. Scarlassara²⁸, R.P. Scharenberg⁸⁸, C. Schiaua⁷⁵, R. Schicker⁸⁷, C. Schmidt⁹⁰, H.R. Schmidt¹¹⁹, S. Schreiner³³, S. Schuchmann⁵⁶, J. Schukraft³³, T. Schuster¹²⁴, Y. Schutz^{33,106}, K. Schwarz⁹⁰, K. Schweda⁹⁰, G. Scioli²³, E. Scomparin¹⁰¹, P.A. Scott⁹⁵, R. Scott¹¹⁶, G. Segato²⁸, I. Selyuzhenkov⁹⁰, S. Senyukov⁶², J. Seo⁸⁹, S. Serici²⁴, E. Serradilla^{10,60}, A. Sevcenco⁵⁴, A. Shabetai¹⁰⁶, G. Shabratova⁶³, R. Shahoyan³³, S. Sharma⁸⁵, N. Sharma^{82,116}, S. Rohni⁸⁵, K. Shigaki⁴³, K. Shtejer⁹, Y. Sibiriak⁹³, M. Siciliano²², E. Sicking⁵⁸, S. Siddhanta¹⁰⁰, T. Siemiarczuk⁷⁴, D. Silvermyr⁷⁹, C. Silvestre⁶⁸, G. Simatovic^{59,91}, G. Simonetti³³, R. Singaraju¹²⁰, R. Singh⁸⁵, S. Singha¹²⁰, V. Singhal¹²⁰, B.C. Sinha¹²⁰, T. Sinha⁹⁴, B. Sitar³⁶, M. Sitta³⁰, T.B. Skaali²¹, K. Skjerdal¹⁸, R. Smakal³⁷, N. Smirnov¹²⁴, R.J.M. Snellings⁴⁹, C. Sogaard^{76,32}, R. Soltz⁷², H. Son²⁰, J. Song⁸⁹, M. Song¹²⁶, C. Soos³³, F. Soramel²⁸, I. Sputowska¹⁰⁸, M. Spyropoulou-Stassinaki⁸³, B.K. Srivastava⁸⁸, J. Stachel⁸⁷, I. Stan⁵⁴, I. Stan⁵⁴, G. Stefanek⁷⁴, M. Steinpreis¹⁹, E. Stenlund³², G. Steyn⁸⁴, J.H. Stiller⁸⁷, D. Stocco¹⁰⁶, M. Stolpovskiy⁴⁷, P. Strmen³⁶, A.A.P. Suaide¹¹¹, M.A. Subieta Vásquez²², T. Sugitate⁴³, C. Suire⁴⁶, R. Sultanov⁵⁰, M. Šumbera⁷⁸, T. Susa⁹¹, T.J.M. Symons⁷¹, A. Szanto de Toledo¹¹¹, I. Szarka³⁶, A. Szczepankiewicz^{108,33}, A. Szostak¹⁸, M. Szymański¹²², J. Takahashi¹¹², J.D. Tapia Takaki⁴⁶, A. Tarantola Peloni⁵⁶, A. Tarazona Martinez³³, A. Tauro³³, G. Tejada Muñoz², A. Telesca³³, C. Terrevoli³¹, J. Thäder⁹⁰, D. Thomas⁴⁹, R. Tieulent¹¹³, A.R. Timmins¹¹⁴, D. Tlusty³⁷, A. Toia^{39,28,99}, H. Torii¹¹⁷, L. Toscano¹⁰¹, V. Trubnikov³, D. Truesdale¹⁹, W.H. Trzaska⁴², T. Tsuji¹¹⁷, A. Tumkin⁹², R. Turrisi⁹⁹, T.S. Tveter²¹, J. Ulery⁵⁶, K. Ullaland¹⁸, J. Ulrich^{65,55}, A. Uras¹¹³, J. Urbán³⁸, G.M. Urciuoli¹⁰³, G.L. Usai²⁴, M. Vajzer^{37,78}, M. Vala^{63,51}, L. Valencia Palomo⁴⁶, S. Vallero⁸⁷, P. Vande Vyvre³³, M. van Leeuwen⁴⁹, L. Vannucci⁷⁰, A. Vargas², R. Varma⁴⁴, M. Vasileiou⁸³, A. Vasiliev⁹³, V. Vechernin¹²¹, M. Veldhoen⁴⁹, M. Venaruzzo²⁵, E. Vercellin²², S. Vergara², R. Vernet⁸, M. Verweij⁴⁹, L. Vickovic¹⁰⁷, G. Viesti²⁸, Z. Vilakazi⁸⁴, O. Villalobos Baillie⁹⁵, A. Vinogradov⁹³, Y. Vinogradov⁹², L. Vinogradov¹²¹, T. Virgili²⁹, Y.P. Viyogi¹²⁰, A. Vodopyanov⁶³, K. Voloshin⁵⁰, S. Voloshin¹²³, G. Volpe³³, B. von Haller³³, I. Vorobyev¹²¹, D. Vranic⁹⁰, J. Vrláková³⁸, B. Vulpescu⁶⁷, A. Vyushin⁹², V. Wagner³⁷, B. Wagner¹⁸, R. Wan⁷, Y. Wang⁷, M. Wang⁷, D. Wang⁷, Y. Wang⁸⁷, K. Watanabe¹¹⁸, M. Weber¹¹⁴, J.P. Wessels^{33,58}, U. Westerhoff⁵⁸, J. Wiechula¹¹⁹, J. Wikne²¹, M. Wilde⁵⁸, G. Wilk⁷⁴, A. Wilk⁵⁸, M.C.S. Williams⁹⁷, B. Windelband⁸⁷, L. Xaplanteris Karampatsos¹⁰⁹, C.G. Yaldo¹²³, Y. Yamaguchi¹¹⁷, S. Yang¹⁸, H. Yang^{14,49}, S. Yasnopolskiy⁹³, J. Yi⁸⁹, Z. Yin⁷, I.-K. Yoo⁸⁹, J. Yoon¹²⁶, W. Yu⁵⁶, X. Yuan⁷, I. Yushmanov⁹³, V. Zaccolo⁷⁶, C. Zach³⁷, C. Zampolli⁹⁷, S. Zaporozhets⁶³, A. Zarochentsev¹²¹, P. Závada⁵³, N. Zaviyalov⁹², H. Zbroszczyk¹²², P. Zelnicek⁵⁵, I.S. Zgura⁵⁴, M. Zhalov⁸⁰, H. Zhang⁷, X. Zhang^{67,7}, F. Zhou⁷, D. Zhou⁷, Y. Zhou⁴⁹, J. Zhu⁷, H. Zhu⁷, J. Zhu⁷, X. Zhu⁷, A. Zichichi^{23,12}, A. Zimmermann⁸⁷, G. Zinovjev³, Y. Zoccarato¹¹³, M. Zynovyev³, M. Zyzak⁵⁶

Affiliation notes

- ⁱ Deceased
- ⁱⁱ Also at: M.V.Lomonosov Moscow State University, D.V.Skobeltzyn Institute of Nuclear Physics, Moscow, Russia
- ⁱⁱⁱ Also at: University of Belgrade, Faculty of Physics and "Vinca" Institute of Nuclear Sciences, Belgrade, Serbia

Collaboration Institutes

- ¹ A. I. Alikhanyan National Science Laboratory (Yerevan Physics Institute) Foundation, Yerevan, Armenia
- ² Benemérita Universidad Autónoma de Puebla, Puebla, Mexico
- ³ Bogolyubov Institute for Theoretical Physics, Kiev, Ukraine
- ⁴ Bose Institute, Department of Physics and Centre for Astroparticle Physics and Space Science (CAPSS), Kolkata, India
- ⁵ Budker Institute for Nuclear Physics, Novosibirsk, Russia
- ⁶ California Polytechnic State University, San Luis Obispo, California, United States
- ⁷ Central China Normal University, Wuhan, China
- ⁸ Centre de Calcul de l'IN2P3, Villeurbanne, France
- ⁹ Centro de Aplicaciones Tecnológicas y Desarrollo Nuclear (CEADEN), Havana, Cuba

- 10 Centro de Investigaciones Energéticas Medioambientales y Tecnológicas (CIEMAT), Madrid, Spain
- 11 Centro de Investigación y de Estudios Avanzados (CINVESTAV), Mexico City and Mérida, Mexico
- 12 Centro Fermi – Centro Studi e Ricerche e Museo Storico della Fisica “Enrico Fermi”, Rome, Italy
- 13 Chicago State University, Chicago, United States
- 14 Commissariat à l’Energie Atomique, IRFU, Saclay, France
- 15 COMSATS Institute of Information Technology (CIIT), Islamabad, Pakistan
- 16 Departamento de Física de Partículas and IGFAE, Universidad de Santiago de Compostela, Santiago de Compostela, Spain
- 17 Department of Physics Aligarh Muslim University, Aligarh, India
- 18 Department of Physics and Technology, University of Bergen, Bergen, Norway
- 19 Department of Physics, Ohio State University, Columbus, Ohio, United States
- 20 Department of Physics, Sejong University, Seoul, South Korea
- 21 Department of Physics, University of Oslo, Oslo, Norway
- 22 Dipartimento di Fisica dell’Università and Sezione INFN, Turin, Italy
- 23 Dipartimento di Fisica dell’Università and Sezione INFN, Bologna, Italy
- 24 Dipartimento di Fisica dell’Università and Sezione INFN, Cagliari, Italy
- 25 Dipartimento di Fisica dell’Università and Sezione INFN, Trieste, Italy
- 26 Dipartimento di Fisica dell’Università ‘La Sapienza’ and Sezione INFN, Rome, Italy
- 27 Dipartimento di Fisica e Astronomia dell’Università and Sezione INFN, Catania, Italy
- 28 Dipartimento di Fisica e Astronomia dell’Università and Sezione INFN, Padova, Italy
- 29 Dipartimento di Fisica ‘E.R. Caianiello’ dell’Università and Gruppo Collegato INFN, Salerno, Italy
- 30 Dipartimento di Scienze e Innovazione Tecnologica dell’Università del Piemonte Orientale and Gruppo Collegato INFN, Alessandria, Italy
- 31 Dipartimento Interateneo di Fisica ‘M. Merlin’ and Sezione INFN, Bari, Italy
- 32 Division of Experimental High Energy Physics, University of Lund, Lund, Sweden
- 33 European Organization for Nuclear Research (CERN), Geneva, Switzerland
- 34 Fachhochschule Köln, Köln, Germany
- 35 Faculty of Engineering, Bergen University College, Bergen, Norway
- 36 Faculty of Mathematics, Physics and Informatics, Comenius University, Bratislava, Slovakia
- 37 Faculty of Nuclear Sciences and Physical Engineering, Czech Technical University in Prague, Prague, Czech Republic
- 38 Faculty of Science, P.J. Šafárik University, Košice, Slovakia
- 39 Frankfurt Institute for Advanced Studies, Johann Wolfgang Goethe-Universität Frankfurt, Frankfurt, Germany
- 40 Gangneung-Wonju National University, Gangneung, South Korea
- 41 Gauhati University, Department of Physics, Guwahati, India
- 42 Helsinki Institute of Physics (HIP) and University of Jyväskylä, Jyväskylä, Finland
- 43 Hiroshima University, Hiroshima, Japan
- 44 Indian Institute of Technology Bombay (IIT), Mumbai, India
- 45 Indian Institute of Technology Indore, Indore, India (IITI)
- 46 Institut de Physique Nucléaire d’Orsay (IPNO), Université Paris-Sud, CNRS-IN2P3, Orsay, France
- 47 Institute for High Energy Physics, Protvino, Russia
- 48 Institute for Nuclear Research, Academy of Sciences, Moscow, Russia
- 49 Nikhef, National Institute for Subatomic Physics and Institute for Subatomic Physics of Utrecht University, Utrecht, Netherlands
- 50 Institute for Theoretical and Experimental Physics, Moscow, Russia
- 51 Institute of Experimental Physics, Slovak Academy of Sciences, Košice, Slovakia
- 52 Institute of Physics, Bhubaneswar, India
- 53 Institute of Physics, Academy of Sciences of the Czech Republic, Prague, Czech Republic
- 54 Institute of Space Sciences (ISS), Bucharest, Romania
- 55 Institut für Informatik, Johann Wolfgang Goethe-Universität Frankfurt, Frankfurt, Germany
- 56 Institut für Kernphysik, Johann Wolfgang Goethe-Universität Frankfurt, Frankfurt, Germany
- 57 Institut für Kernphysik, Technische Universität Darmstadt, Darmstadt, Germany
- 58 Institut für Kernphysik, Westfälische Wilhelms-Universität Münster, Münster, Germany
- 59 Instituto de Ciencias Nucleares, Universidad Nacional Autónoma de México, Mexico City, Mexico
- 60 Instituto de Física, Universidad Nacional Autónoma de México, Mexico City, Mexico

- 61 Institut of Theoretical Physics, University of Wrocław
- 62 Institut Pluridisciplinaire Hubert Curien (IPHC), Université de Strasbourg, CNRS-IN2P3, Strasbourg, France
- 63 Joint Institute for Nuclear Research (JINR), Dubna, Russia
- 64 KFKI Research Institute for Particle and Nuclear Physics, Hungarian Academy of Sciences, Budapest, Hungary
- 65 Kirchhoff-Institut für Physik, Ruprecht-Karls-Universität Heidelberg, Heidelberg, Germany
- 66 Korea Institute of Science and Technology Information, Daejeon, South Korea
- 67 Laboratoire de Physique Corpusculaire (LPC), Clermont Université, Université Blaise Pascal, CNRS–IN2P3, Clermont-Ferrand, France
- 68 Laboratoire de Physique Subatomique et de Cosmologie (LPSC), Université Joseph Fourier, CNRS-IN2P3, Institut Polytechnique de Grenoble, Grenoble, France
- 69 Laboratori Nazionali di Frascati, INFN, Frascati, Italy
- 70 Laboratori Nazionali di Legnaro, INFN, Legnaro, Italy
- 71 Lawrence Berkeley National Laboratory, Berkeley, California, United States
- 72 Lawrence Livermore National Laboratory, Livermore, California, United States
- 73 Moscow Engineering Physics Institute, Moscow, Russia
- 74 National Centre for Nuclear Studies, Warsaw, Poland
- 75 National Institute for Physics and Nuclear Engineering, Bucharest, Romania
- 76 Niels Bohr Institute, University of Copenhagen, Copenhagen, Denmark
- 77 Nikhef, National Institute for Subatomic Physics, Amsterdam, Netherlands
- 78 Nuclear Physics Institute, Academy of Sciences of the Czech Republic, Řež u Prahy, Czech Republic
- 79 Oak Ridge National Laboratory, Oak Ridge, Tennessee, United States
- 80 Petersburg Nuclear Physics Institute, Gatchina, Russia
- 81 Physics Department, Creighton University, Omaha, Nebraska, United States
- 82 Physics Department, Panjab University, Chandigarh, India
- 83 Physics Department, University of Athens, Athens, Greece
- 84 Physics Department, University of Cape Town and iThemba LABS, National Research Foundation, Somerset West, South Africa
- 85 Physics Department, University of Jammu, Jammu, India
- 86 Physics Department, University of Rajasthan, Jaipur, India
- 87 Physikalisches Institut, Ruprecht-Karls-Universität Heidelberg, Heidelberg, Germany
- 88 Purdue University, West Lafayette, Indiana, United States
- 89 Pusan National University, Pusan, South Korea
- 90 Research Division and ExtreMe Matter Institute EMMI, GSI Helmholtzzentrum für Schwerionenforschung, Darmstadt, Germany
- 91 Rudjer Bošković Institute, Zagreb, Croatia
- 92 Russian Federal Nuclear Center (VNIIEF), Sarov, Russia
- 93 Russian Research Centre Kurchatov Institute, Moscow, Russia
- 94 Saha Institute of Nuclear Physics, Kolkata, India
- 95 School of Physics and Astronomy, University of Birmingham, Birmingham, United Kingdom
- 96 Sección Física, Departamento de Ciencias, Pontificia Universidad Católica del Perú, Lima, Peru
- 97 Sezione INFN, Bologna, Italy
- 98 Sezione INFN, Catania, Italy
- 99 Sezione INFN, Padova, Italy
- 100 Sezione INFN, Cagliari, Italy
- 101 Sezione INFN, Turin, Italy
- 102 Sezione INFN, Trieste, Italy
- 103 Sezione INFN, Rome, Italy
- 104 Sezione INFN, Bari, Italy
- 105 Nuclear Physics Group, STFC Daresbury Laboratory, Daresbury, United Kingdom
- 106 SUBATECH, Ecole des Mines de Nantes, Université de Nantes, CNRS-IN2P3, Nantes, France
- 107 Technical University of Split FESB, Split, Croatia
- 108 The Henryk Niewodniczanski Institute of Nuclear Physics, Polish Academy of Sciences, Cracow, Poland
- 109 The University of Texas at Austin, Physics Department, Austin, TX, United States
- 110 Universidad Autónoma de Sinaloa, Culiacán, Mexico

- 111 Universidade de São Paulo (USP), São Paulo, Brazil
- 112 Universidade Estadual de Campinas (UNICAMP), Campinas, Brazil
- 113 Université de Lyon, Université Lyon 1, CNRS/IN2P3, IPN-Lyon, Villeurbanne, France
- 114 University of Houston, Houston, Texas, United States
- 115 University of Technology and Austrian Academy of Sciences, Vienna, Austria
- 116 University of Tennessee, Knoxville, Tennessee, United States
- 117 University of Tokyo, Tokyo, Japan
- 118 University of Tsukuba, Tsukuba, Japan
- 119 Eberhard Karls Universität Tübingen, Tübingen, Germany
- 120 Variable Energy Cyclotron Centre, Kolkata, India
- 121 V. Fock Institute for Physics, St. Petersburg State University, St. Petersburg, Russia
- 122 Warsaw University of Technology, Warsaw, Poland
- 123 Wayne State University, Detroit, Michigan, United States
- 124 Yale University, New Haven, Connecticut, United States
- 125 Yildiz Technical University, Istanbul, Turkey
- 126 Yonsei University, Seoul, South Korea
- 127 Zentrum für Technologietransfer und Telekommunikation (ZTT), Fachhochschule Worms, Worms, Germany